Colloids and Surfaces B: Biointerfaces 112 (2013) 310–314

Contents lists available at ScienceDirect

Colloids and Surfaces B: Biointerfaces

journal homepage: www.elsevier.com/locate/colsurfb

Gold nanoparticles coated polystyrene/reduced graphite oxide microspheres with improved dispersibility and electrical conductivity for dopamine detection

Tao Qian, Chenfei Yu, Shishan Wu*, Jian Shen

School of Chemistry and Chemical Engineering, Nanjing University, Nanjing 210093, China

ARTICLE INFO

Article history:
Received 12 June 2013
Received in revised form 1 August 2013
Accepted 7 August 2013
Available online xxx

Keywords:
Gold nanoparticles
Reduced graphite oxide
Polystyrene
Biosensor
Dispersibility

ABSTRACT

Gold nanoparticles coated polystyrene/reduced graphite oxide (AuNPs@PS/RGO) microspheres have been successfully prepared via a facile process, and the decorative gold nanoparticles could prevent the aggregation of RGO by electrostatic repulsive interaction, and lead to high dispersibility of the composite. The prepared composite has a highly increased conductivity of 129 S m^{-1} due to the unique electrical properties of citrate reduced gold nanoparticles. Being employed as an electrochemical sensor for detection of dopamine, the modified electrode exhibits remarkable sensitivity (3.44 μA/μM) and lower detection limit (5 nM), with linear response in a range of 0.05–20 μM. Moreover, valid response to dopamine obtained in present work also indicates the prospective performances of AuNPs@PS/RGO microspheres to other biological molecules, such as nucleic acids, proteins and enzymes.

1. Introduction

Dopamine (DA), as one of the important neurotransmitters, plays a significant role in the function of human metabolism, cardiovascular, central nervous, renal, and hormonal systems [1]. Alterations in DA contribute to the development of a number of severe mental illnesses, such as Parkinson's disease, Schizophrenia and depression [2–4]. The determination of DA has been reported using electrophoresis [5], chromatography [6], high performance liquid chromatography [7], flow injection chemiluminescence [8] and spectrophotometry [9]. Although these methods can offer good selectivity and detection limit, they often are cost intensive, time consuming, qualified personnel and complex pre-treatment steps. Accordingly, it still remains a great challenge to develop a suitable analytical technique to detect DA. Electrochemical oxidation of DA is possible at unmodified electrodes; however, disadvantages, such as fouling of the electrode surface due to oxidation products and interference from co-oxidation of ascorbic acid (AA) and uric acid (UA) present in biological fluids in the same potential window have been of concern. Hence it is important to design electrodes that are specific, selective and sensitive toward this analyte.

Carbon nanomaterials are proved to be among the outstanding candidates as novel platforms for sensing because their bio-electrocatalytic properties, chemical functionalities, and physical stability can be quite easily tailored. Among them, graphene has been particularly attractive as novel platform for DA sensing [10–14]. Reduced graphite oxide (RGO), one kind of chemically derived graphene, has shown similar characteristics to graphene in many aspects. It is noted that RGO, which have high specific surface area, tend to form irreversible agglomerates or even to restack to form graphite through strong π–π stacking and van der Waals interaction [15]. Hence the prevention of aggregation is a key challenge in the synthesis and processing of bulk-quantity RGO.

An ideal graphene/polymer composite would consist of RGO sheets and the polymer separating them in order to improve the dispersibility of RGO, and thereby maximizing property enhancement [16,17]. The specific polymer system chosen for this study is polystyrene (PS). Nonconducting polystyrene microspheres are served as templates for preparing PS/RGO core/shell composite, which can expand the specific surface area of RGO and overcome its aggregation, thus promote electrocatalysis performance. However, the electrical conductivity of the composite is still undesirable due to the nonconducting polystyrene core, and the dispersibility is also unsatisfactory.

Noble metal-nanoparticles, especially gold nanoparticles (AuNPs), are paid intensive scientific and technological attentions as they have unique chemical, electrical and optical properties. Catalytic activity of AuNPs is widely reported about their extraordinary contribution in facilitating the electron transfer and decreasing the over-potential of important reactions [18–23].

* Corresponding author. Tel.: +86 83316661; fax: +86 83316661.
E-mail address: shishanwu@nju.edu.cn (S. Wu).

0927-7765/$ – see front matter © 2013 Elsevier B.V. All rights reserved.
http://dx.doi.org/10.1016/j.colsurfb.2013.08.005

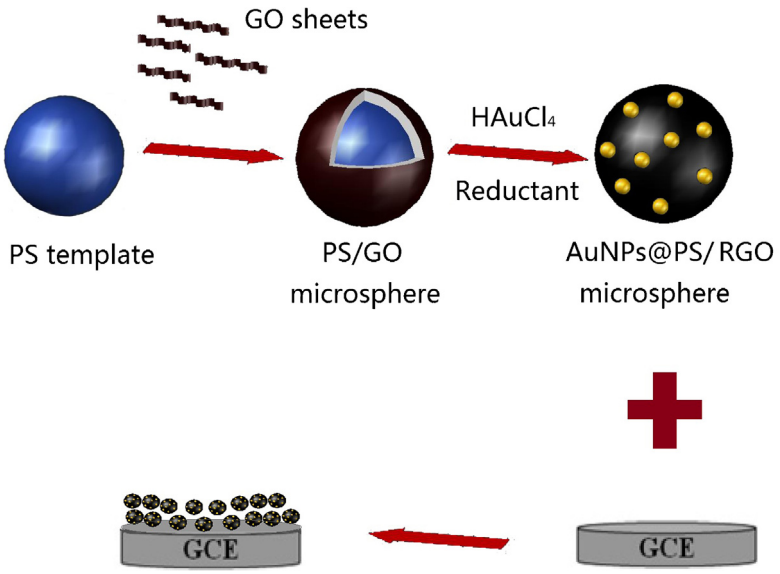

Fig. 1. Scheme showing the chemical route to the synthesis of AuNPs@PS/RGO.

AuNPs prepared by the citrate reduction method are negatively charged due to citrate capping effect and stable with the assistance of electrostatic repulsion [24]. When probe molecules with positive amine groups are added into colloidal AuNPs, they are adsorbed onto the surface of the nanoparticles, which significantly enhance the electrochemical sensibility. In this work, PS/GO core/shell microspheres are served as templates and mixed with $AuCl_4$ in aqueous solution, the mixtures are then reduced by reductant together. The facile fabrication of AuNPs on the surface of PS/RGO core/shell microspheres (Fig. 1) could significantly enhance the dispersibility, electrical conductivity of the composite, and improve the sensibility of electrochemical detection for DA due to the unique chemical, electrical properties of citrate reduced AuNPs.

2. Materials and methods

2.1. Materials

Styrene (St) and hydrazine hydrate (80%, AR) were purchased from Shanghai Chemical Reagent Co. (China). AIBA (2, 2′-azobis[2-methylpropionamidine] dihydrochloride), and polyvinylpyrrolidone (PVP) were purchased from Tianjin Chemical Reagent Co. (China). $HAuCl_4$, DA, AA, and UA were purchased from aladdin Chemical Reagent Co. (China).

2.2. Apparatus

High-resolution transmission electron microscope (HRTEM) images were taken in a FEI Tecnai F30 operated at 200 kV. Energy dispersive X-ray spectroscopy (EDS) was conducted by EDS-integrated Hitachi S-4800 (Hitachi, Japan). X-ray powder diffraction (XRD) analysis was performed on a Shimadzu XRD 6000 diffractometer (Japan). Scanning electron microscope (SEM) images were collected on Hitachi S-4800 (Japan). Zeta potential was recorded on a Malvern Nano-Z Instrument (UK). The electrical conductivity of all synthesized materials at room temperature was determined using the four-probe system connected to a Keithley 2400 source meter. All electrochemical measurements were carried out with a CHI660D (Shanghai CH Instrument Company, China). Cyclic voltammetry (CV) and Differential pulse voltammetry (DPV) were performed with a conventional three-electrode system consisting of a bare or modified glassy carbon electrode (GCE; diameter = 3 mm) as the working electrode, a saturated calomel electrode (SCE) as the reference electrode, and a platinum wire as the counter electrode.

2.3. Synthesis method

GO was synthesized from graphite powder by a modified Hummers method and dispersed in water with the concentration of 1.0 mg/1.0 g H_2O by ultrasonication. The monodisperse PS microspheres in the size of 280 nm were prepared by emulsifier-free emulsion polymerization as follows: styrene (10.00 g), PVP (0.40 g) and H_2O (80.00 g) were slowly heated to 70 °C in N_2 environment. AIBA aqueous solution (0.06 wt%, 10.00 g) was added, and the reaction was carried out at 70 °C for 18 h. The procedure to prepare PS/GO microspheres are the follows: PS (1.00 g) microspheres were dispersed in water (80.00 mL), heated to 70 °C, and 20 mL GO dispersion was dropped into the solution at the speed of 2.5 mL/h. A precipitate was formed and collected by centrifugation, then dried under vacuum for 24 h. The preparation of the AuNPs@PS/RGO composite is depicted in Fig. 1. The PS/GO microspheres (0.25 g) were dispersed in water (25 mL) with ultrasonication. 0.5 mL $HAuCl_4$ solution (1.0 wt%) was added. The dispersion was heated to 100 °C, 0.5 mL of the tri-sodium citrate (100 mM), 4.0 mL $NaBH_4$ (50 mM) and 1.00 mL hydrazine hydrate were added into the solution under stirring. After continuously stirred for 1 h under 100 °C, the resulting AuNPs@PS/RGO microspheres were collected by centrifugation and dried under vacuum for 24 h.

2.4. Fabrication of the modified electrode

A GCE was carefully polished with 0.3 μm and 0.05 μm alumina slurry on micro-cloth pads, rinsed thoroughly with three-distilled water between each polishing step, then cleaned successively with three distilled water, anhydrous ethanol and three distilled water in an ultrasonic bath. The modified GCE was prepared by adding a drop (14 μL) of the mixture solution described previously directly to the top of the electrode. The solvent was allowed to evaporate at infrared lamp. The sensor was stored under 4 °C for further investigations.

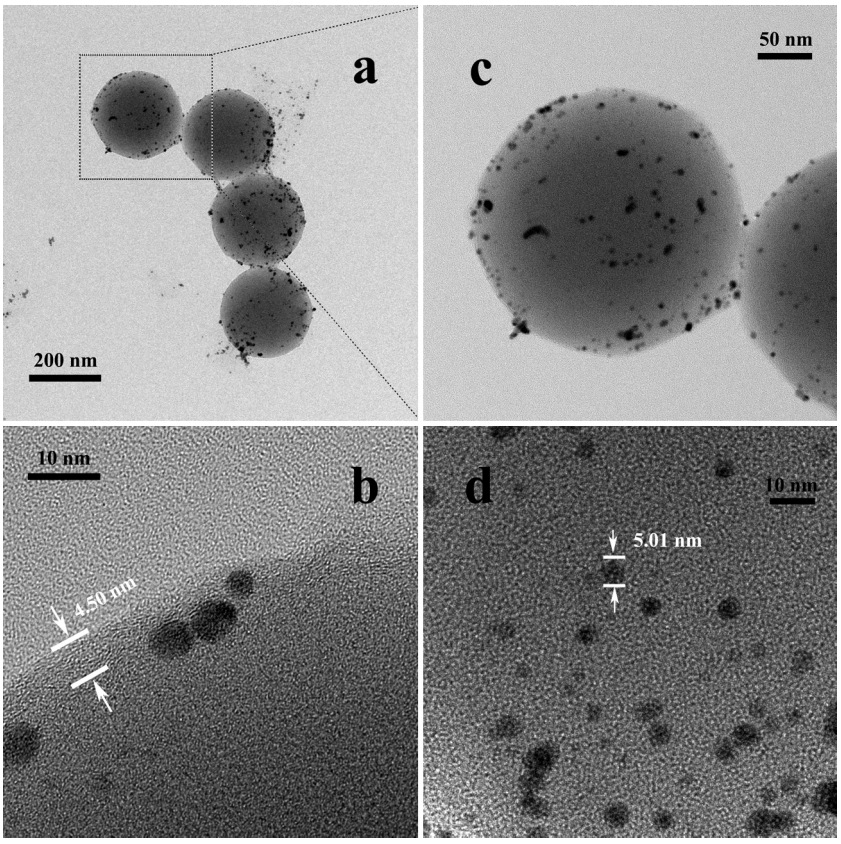

Fig. 2. HRTEM images of (a) AuNPs@PS/RGO microspheres, (b–d) AuNPs@PS/RGO microspheres with partial enlarged.

3. Results and discussion

3.1. Characterization of AuNPs@PS/RGO microspheres

The surface morphology of the composite material was examined through SEM (Please refer to supplementary material Fig. S1) and HRTEM (Fig. 2). The SEM images of AuNPs@PS/RGO indicate that prepared composite exclusively consists of a large quantity of uniform microspheres, which are well-separated from each other with diameters ranging from 200 to 220 nm. The morphology of RGO that are coated on PS microspheres shows smooth and complete surface with a thickness about 4.50 nm (Fig. 2b). More details are presented by the HRTEM images with partial enlarged (Fig. 2c and d), which show the AuNPs coated on the surface of PS/RGO microspheres are high-dense and uniform (Fig. 2c) with a average scale of approximately 5 nm (Fig. 2d).

EDS image of the hybrids indicates the presence of C (0.028 keV), O (0.054 keV), Au (0.215 and 0.974 keV), (Fig. 3). The O signal is extremely weak and nearly disappeared, suggesting that GO shell is mostly reduced to RGO. The intense Au signal indicates that the AuNPs are high-density coated on the PS/RGO microspheres. The structure of the composite was further examined by XRD (Fig. 4). The characteristic peak of graphite (curve a) focuses at 26.5° (2θ). Once the graphite is oxidized, the characteristic peak of GO (curve b) appears at 10.4°. After being coated on the PS microspheres (PS/GO) (curve d), the characteristic peak of GO strengthens the characteristic peak of PS (curve c) microspheres at approximately 10.4°. As for the AuNPs@PS/RGO (curve e) microspheres, a broad peak presents at 23.3° corresponding to RGO is observed, also the characteristic peak of GO at 10.4° disappears, which means that most of the GO has been reduce. The Bragg angles of 38.1°, 44.3°, 64.9° and 77.4° are clearly observed, which could be indexed to the (1 1 1), (2 0 0), (2 2 0) and (3 1 1) planes of the AuNPs.

3.2. Comparison of dispersion among RGO, PS/RGO and AuNPs@PS/RGO microspheres

For proving that the dispersion of AuNPs@PS/RGO microspheres in water is superior to RGO, the dispersion of RGO, PS/RGO, and AuNPs@PS/RGO microspheres were investigated by standing for 3 h after ultrasonication. As can be seen in supplementary material Fig. S2, RGO are absolutely aggregated and floated on top of aqueous phase; few amount of PS/RGO microspheres are dispersed in water, and most part are separated with aqueous phase; AuNPs@PS/RGO microspheres could easily be suspended in water and retain a homogeneous black aqueous dispersion after 3 h. Such

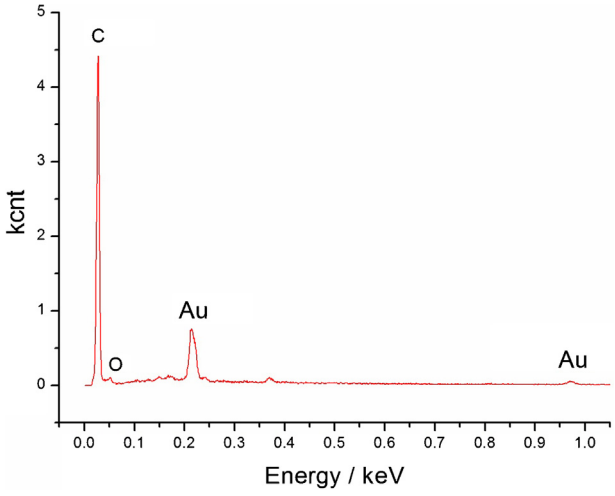

Fig. 3. EDS image of AuNPs@PS/RGO microspheres.

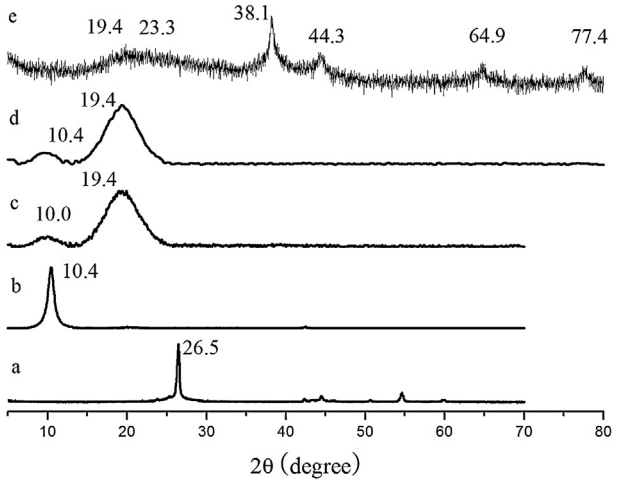

Fig. 4. XRD patterns of (a) graphite (b) GO (c) PS (d) PS/GO and (e) AuNPs@PS/RGO.

homogeneous suspension is fairly stable and no sign of coagulation can be observed even after more than 60 days storage. The negative charge of decorative AuNPs could be a contributing factor in disperse progress of the prepared composite which is consistent with the results of zeta potentials (please refer to supplementary material Table S1). Hence it can stay at the electrode surface and sustain a good stability after a series of repeating tests even without the help of nafion or chitosan. The excellent dispersibility can broaden the application of AuNPs@PS/RGO in biological and chemical analysis.

3.3. Comparison of electrical conductivity among RGO, PS/RGO and AuNPs@PS/RGO microspheres

The electrical conductivities of all synthesized materials were determined using the four-probe system at room temperature. The conductivity of the bare polymer is very low (below the lower limitation of the instrument) and hence we could not get any data for this sample. Similar results have been reported about the electrical conductivity of this polymer in previous studies [25,26]. The electrical conductivity of PS/RGO is 0.56 S m^{-1}. The AuNPs@PS/RGO has a much higher conductivity of 129 S m^{-1} in comparison to PS/RGO and some previous works (graphene nanosheets–polystyrene nanocomposites [27], 0.029 S m^{-1}; PS/graphene nanocomposites [28], 3.49 S m^{-1}; polystyrene-chemically converted graphene composite [17], 72.2 S m^{-1}). These experimental results demonstrate that AuNPs can efficaciously increase the electrical conductivity of the nanocomposite.

3.4. Optimization of the experimental conditions

The electrocatalytic activity of the AuNPs@PS/RGO microspheres modified GCE toward DA was compared with bare GCE by investigation of CV (please refer to supplementary material Fig. S3). The sensor triggers an electrocatalytic reaction with addition of DA, both the bare GCE and modified GCE exhibits electrocatalytical oxidation response. In the case of bare GCE, the oxidation of DA results in a broad peak with the peak potential of 0.331 V, however, the AuNPs@PS/RGO microspheres doped GCE exhibits a lower oxidation peak potential at 0.276 V with a pronounced current signal, indicating that AuNPs@PS/RGO microspheres have excellent electrocatalytic activity for DA oxidation.

The CV curves of DA at the AuNPs@PS/RGO microspheres were investigated at different scan rate (Please refer to supplementary material Fig. S4a). With the increase of scan rate, the peak current of DA increased. Supplementary material Fig. S4b shows a linear response of the anodic peak current ($R = 0.9995$) and cathodic peak current ($R = 0.9982$) versus the scan rate and this implies a surface absorption-controlled process.

As shown in supplementary material Fig. S5a, the maximum redox current is obtained at pH 6.5. In addition, we explored the relationship between peak potential of DA and pH (please refer to supplementary material Fig. S5b). The anodic peak potential is proportional to the pH (with $R = 0.9986$), indicating that the electron transfer step is preceded by a protonation with the same number of protons involved in the DA oxidation mechanism.

3.5. Quantitative determination of DA by DPV

Differential pulse voltammetry (DPV) can provide better peak resolution and higher current sensitivity. The quantitative analysis of DA was investigated by DPV instead of CV under the selected conditions. Fig. 5A shows DPV curves of different concentrations of DA on AuNPs@PS/RGO modified GCE. A good linear region with a concentration of DA in the range 0.05–20 μM is shown in Fig. 5B, line a. The linear relation has a regression equation of I_{pa} (μA) = 0.48+3.44C_{DA} (μM) with a correlation coefficient of 0.9990. When the signal to noise ratio is 3 (S/N = 3), a detection limit as low as 5 nM is observed. Compared with polystyrene-grafted-RGO hybrid [29] (slope: 0.336) and PS/RGO (slope: 2.07, Fig. 5B, line b) modified electrode, the slope of the calibration plot in the present work is much higher, and the detection limit of the present system is much lower. As shown in supplementary material Table S2, the result of AuNPs@PS/RGO composite modified GCE detection platform is compared with other published works. It is obvious that the prepared sensor is more sensitive, and has a lower detection limit

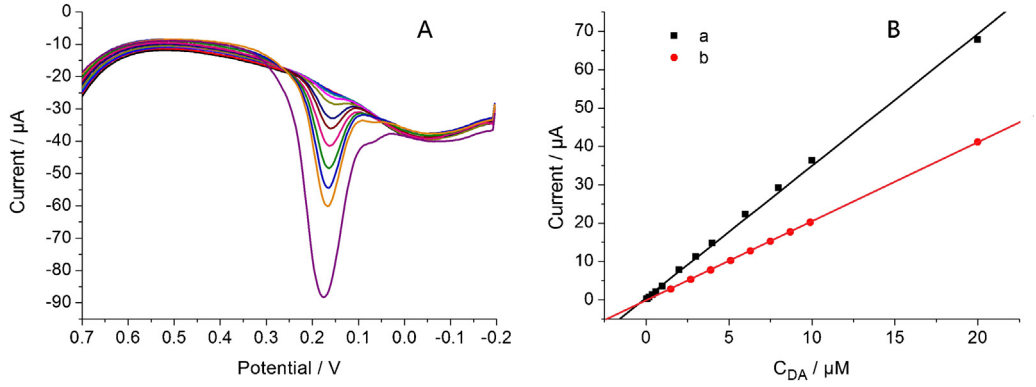

Fig. 5. (A) The DPVs of increasing DA concentration in 0.1 M PBS (pH = 6.5), DA concentration was 0.05, 0.1, 0.2, 0.4, 0.6, 1, 2, 3, 4, 6, 8, 10, and 20 μM (from top to bottom), respectively. (B) The calibration curve of DA obtained with (a) AuNPs@PS/RGO, and (b) PS/RGO modified GCE.

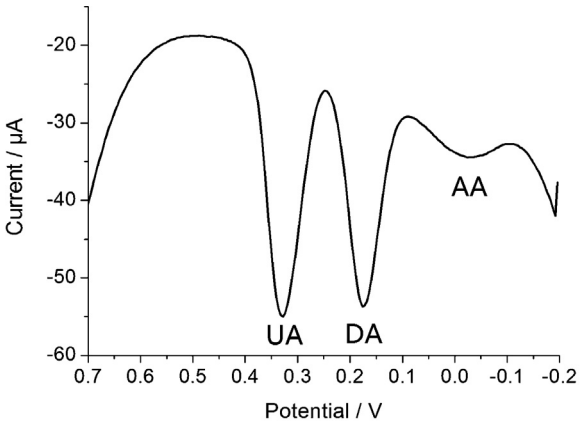

Fig. 6. The DPVs of AuNPs@PS/RGO microspheres modified GCE toward 10 μM DA in the present of 125 μM AA and 330 μM UA (an environment similar to human blood serum).

toward DA, which provides an attractive perspective for its wide application.

3.6. Selective determination of DA in the presence of UA and AA

As is known, some coexisted electroactive biomolecules (UA, and AA, etc.) generally show the serious interference for electrochemical detection of DA, which limit the real application of the sensor. Fig. 6 shows the results of DPV responses of DA at AuNPs@PS/RGO microspheres modified GCE. The figure demonstrates that the responses to DA, AA, and UA at the AuNPs@PS/RGO microspheres modified GCE are relatively independent, and the oxidation peaks for DA can be clearly identified at about 0.18 V in an environment similar to human blood serum, while the oxidation peak potentials of AA and UA are located at −0.02 and 0.33 V, respectively. That is to say, the electrode presented here has a good selectivity with a decent sensitivity using DPV technique for DA detection.

3.7. Stability and reproducibility of AuNPs-PS/RGO microspheres modified GCE

The reproducibility of the prepared sensor was evaluated using the following method. Five proposed prepared sensors were incubated with 1 μmol/L DA, all electrodes exhibits similar electrochemical responses and the relative standard deviation (RSD) of 3.5%. This demonstrates that the reproducibility of the proposed sensor for DA detection is acceptable. The stability of prepared sensor was studied through measuring the current responses of the prepared sensor after long-term storage every 2 days for a long time. It retains 93% of its initial response after a storage period of 10 days, which indicates that the prepared sensor has good stability.

4. Conclusion

In conclusion, AuNPs@PS/RGO composite has been successfully prepared, and the decorative AuNPs could prevent the aggregation of RGO by electrostatic repulsive interaction, which lead to a high dispersibility of the composite. Furthermore, the conductivity of the prepared composite can be significantly enhanced by fabrication of AuNPs. The electrochemical test results show that the AuNPs@PS/RGO composite modified electrode exhibits excellent sensitivity and selectivity response for dopamine. Moreover, this electrochemical biosensor is suitable for building a broader application of various types of biological molecules and easy to achieve, which might provide a promising potential for practical application in biological or clinical target analysis.

Acknowledgments

This work was supported by the Foundation of Jiangsu Collaborative Innovation Center of Biomedical Functional Materials.

Appendix A. Supplementary data

Supplementary data associated with this article can be found, in the online version, at http://dx.doi.org/10.1016/j.colsurfb.2013.08.005.

References

[1] M.L.A.V. Heien, A.S. Khan, J.L. Ariansen, J.F. Cheer, P.E.M. Phillips, K.M. Wassum, R.M. Wightman, Proc. Natl. Acad. Sci. U. S. A 102 (2005) 10023.
[2] K.A. Conway, Science 294 (2001) 1346.
[3] B. Rubi, P. Maechler, Endocrinology 151 (2010) 5570.
[4] A. Zhang, J.L. Neumeyer, R.J. Baldessarini, Chem. Rev. 107 (2007) 274.
[5] A.J. Wang, J.J. Feng, W.J. Dong, Y.H. Lu, Z.H. Li, M.L. Riekkola, J. Chromatogr. A 1217 (2010) 5130.
[6] P. Uutela, R. Reinila, K. Harju, P. Piepponen, R.A. Ketola, R. Kostiainen, Anal. Chem. 81 (2009) 8417.
[7] N. Li, J. Guo, B. Liu, Y. Yu, H. Cui, L. Mao, Y. Lin, Anal. Chim. Acta 645 (2009) 48.
[8] S. Zhao, Y. Huang, M. Shi, R. Liu, Y.M. Liu, Anal. Chem. 82 (2012) 2036.
[9] J.J. Feng, H. Guo, Y.F. Li, Y.H. Wang, W.Y. Chen, A.J. Wang, ACS Appl. Mater. Interfaces 5 (2013) 1226.
[10] C. Sun, H. Lee, J. Yang, C. Wu, Biosens. Bioelectron. 26 (2011) 3450.
[11] K.J. Huang, Q.S. Jing, Z.W. Wua, L. Wang, C.Y. Wei, Colloids Surf. B 88 (2011) 310.
[12] Y. Fan, H.T. Lu, J.H. Liu, C.P. Yang, Q.S. Jing, Y.X. Zhang, X.K. Yang, K.J. Huang, Colloids Surf. B 83 (2011) 78.
[13] S.J. Li, J.Z. He, M.J. Zhang, R.X. Zhang, X.L. Lv, S.H. Li, H. Pang, Electrochim. Acta 102 (2013) 58.
[14] S.J. Li, D.H. Deng, Q. Shi, S.R. Liu, Microchim. Acta 177 (2012) 325.
[15] D. Li, M.B. Muller, D. Gilje, R.B. Kaner, G.G. Wallace, Nat. Nanotechnol. 3 (2008) 101.
[16] H. Kim, H.T. Hahn, L.M. Viculis, S. Gilje, R.B. Kaner, Carbon 45 (2007) 1578.
[17] X.Y. Qi, D. Yan, Z.G. Jiang, Y.K. Cao, Z.Z. Yu, F. Yavari, N. Koratkar, ACS Appl. Mater. Interfaces 3 (2011) 3130.
[18] S. Bharathi, M. Nogami, S. Ikeda, Langmuir 17 (2001) 1.
[19] C.R. Raj, T. Okajima, T.J. Ohsaka, Electroanal. Chem. 543 (2003) 127.
[20] A.N. Shipway, M. Lahav, I. Willner, Adv. Mater. 12 (2000) 993.
[21] C.F. Ou, R. Yuan, Y.Q. Chai, M.Y. Tang, R. Chai, X.L. He, Anal. Chim. Acta 603 (2007) 205.
[22] C.L. Xiang, Y.J. Zhou, L.X. Sun, F. Xu, Talanta 74 (2007) 206.
[23] L. Wang, E.K. Wang, Electrochem. Commun. 6 (2004) 49.
[24] R.A. Puebla, E. Arceo, P.G. Goulet, J. Garrido, R.F. Aroca, J. Phys. Chem. B 109 (2005) 3787.
[25] J. Yu, K. Lu, E. Sourty, N. Grossiord, C.E. Koning, J. Loos, Carbon 45 (2007) 2897.
[26] X.Y. Qi, D. Yan, Z. Jiang, Y.K. Cao, Z.Z. Yu, F. Yavari, N. Koratkar, ACS Appl. Mater. Interfaces 3 (2011) 3130.
[27] V.H. Pham, T.V. Cuong, T.T. Dang, S.H. Hur, B.S. Kong, E.J. Kim, E.W. Shin, J.S. Chung, J. Mater. Chem. 21 (2011) 11312.
[28] H.T. Hu, X.B. Wang, J.C. Wang, L. Wan, F.M. Liu, H. Zheng, R. Chen, C.H. Xu, Chem. Phys. Lett. 484 (2010) 247.
[29] W.J. Liu, J. Xiao, C.S. Wang, H.Y. Yin, H.F. Xie, R.S. Cheng, Mater. Lett. 100 (2013) 70.